sustainability

MDPI

Article

Hydrogen vs. Battery-Based Propulsion Systems in Unipersonal Vehicles—Developing Solutions to Improve the Sustainability of Urban Mobility

F. Isorna Llerena [1,*], E. López González [1], J. J. Caparrós Mancera [1], F. Segura Manzano [2] and J. M. Andújar [2]

[1] Instituto Nacional de Técnica Aeroespacial (INTA), Área de Energía. Ctra. Huelva-Matalascañas, km. 34. Mazagón, 21130 Huelva, Spain; lopezge@inta.es (E.L.G.); jcapman@inta.es (J.J.C.M.)
[2] Centro de Investigación en Tecnología, Energía y Sostenibilidad (CITES), Universidad de Huelva, 21007 Huelva, Spain; francisca.segura@diesia.uhu.es (F.S.M.); andujar@diesia.uhu.es (J.M.A.)
* Correspondence: isornaf@inta.es; Tel.: +34-959208847

Abstract: The percentage of the population in urban areas has increased by ten points from 2000 (46%) to 2020 (56%); it is expected to reach up to 70% by 2050. This undoubtedly will encourage society to use alternative transports. On the other hand, the widespread fear of pandemics seems to be here to stay, and it is causing most people to leave public transport to use private cars, and a few have chosen unipersonal electric vehicles. As a consequence, the decision of using private cars negatively affects the air quality, and consequently urban population health. This paper aims to demonstrate a sustainable solution for urban mobility based on a hydrogen powered unipersonal electric vehicle, which, as shown, provides great advantages over the conventional battery powered unipersonal electric vehicle. To show this, the authors have developed both vehicles in comparable versions, using the same platform, and ensuring that the total weight of the unipersonal electric vehicle was the same in both cases. They have been subjected to experimental tests that support the features of the hydrogen-based configuration versus the battery-based one, including higher specific energy, more autonomy, and shorter recharge time.

Keywords: sustainable urban mobility; unipersonal hydrogen-based electric vehicle; unipersonal battery-based electric vehicle; experimental comparison

Citation: Isorna Llerena, F.; López González, E.; Caparrós Mancera, J.J.; Segura Manzano, F.; Andújar, J.M. Hydrogen vs. Battery-Based Propulsion Systems in Unipersonal Vehicles—Developing Solutions to Improve the Sustainability of Urban Mobility. *Sustainability* **2021**, *13*, 5721. https://doi.org/10.3390/su13105721

Academic Editor: Tomonobu Senjyu

Received: 29 April 2021
Accepted: 17 May 2021
Published: 20 May 2021

1. Introduction

According to the World Data Bank [1], the percentage of urban population has increased by 10 points in the 21st century (in 2000, the urban population was 46%, and in 2020 it reached 56%), and it is expected to reach 70% by 2050. This undoubtedly forces cities to undertake a sustainable transformation of their urban model, and society to use alternative transports. Although public transport plays an important role, a recent analysis has quantified a 60% decrease in public ridership due to the COVID-19 pandemic [2]. Most people have swapped public transport for private cars, and few have chosen the bike. This decision, widely extended across society, negatively affects the air quality and, consequently, urban population health [3].

Therefore, in these times in which people receive daily instruction to avoid social interaction (fear of sharing with another person) while humanity must continue to preserve sustainability and respect for the environment, it is crucial to develop urban transport solutions that guarantee the ineviTable 1.5 m physical distance while preserving our planet. In this sense, battery-powered unipersonal vehicles show some challenges not yet resolved. Firstly, the batteries are heavy and have great proportions, in terms of limited specific power [4]. Regarding autonomy, specific energy can also be limiting with respect to interurban mobility. Batteries also have considerable degradation during their lifetime. This implies a lower performance in the electric vehicles over time [5,6]. Additionally, with

the increased use of electric vehicles, a large number of batteries is required to be produced. However, the raw materials, such as lithium, are limited, and recycling will not be enough to continue supplying lithium in a few decades. It would not make sense to repeat the political and economic fights regarding fossil fuels to new materials [7]. Additionally, safety issues must also be taken into account; in recent years, there have been numerous cases of Li-ion battery fires and explosions, resulting in property damage and bodily injuries [8–10]. On the other hand, the design and fabrication of new sustainable electrode materials is taking on greater importance in recent years, so that they may be used as a substitute for traditional raw materials [11,12].

Thus, sustainable alternatives with hydrogen as the energy carrier, obtained from renewable energy [13], are being considered for urban mobility in electric unipersonal vehicles [14–18]. Hydrogen-powered unipersonal electric vehicles offer advantages such as fast charging, long range and low on-board pressure. Pressure tanks are the best option for the hydrogen delivery when low hydrogen demand is needed, and the distances are short between hydrogen production and delivery sites [19].

Comparing the behavior of battery-powered unipersonal electric vehicles versus hydrogen-powered unipersonal electric vehicles, this work presents the advantages in terms of high efficiency, high power density, fast start-up and response to load changes, and long life in favor of the latter. However, there are also disadvantages, such as the current cost of hydrogen technology and the availability of recharging points. As far as technological development is concerned, and in comparison with previous scientific works found in the literature, this paper presents important novelties such as the specific design of the test platform, the use of comparable propulsion systems and real tests in a controllable urban circuit [20–23].

Table 1 shows the main conclusions obtained from the scientific literature. The different technological configurations include the use of batteries, as well as the use of hydrogen through fuel cells (FCs), solar propulsion and various combinations. In comparison to these works, this paper makes a proposal for sustainable urban mobility in which two technologies, battery and the hybridization of battery + hydrogen, are compared, obtaining a scalable model with great autonomy and fast recharge.

Table 1. Comparison of the proposed paper's findings with previous scientific works.

Reference	Powertrain	Nominal Power	Autonomy (km)	Recharge Time	Weight (kg)	On-Road Test	Velocity (m/s)
Authors' proposal	BAT + H2	250	290	1.8 min	33	Yes	3.33
[20]	PV + BAT	800	37	8 h	85	Yes	5.39
[21]	H2	300	800	-	65	No	12.5
[23]	BAT + H2	5000	-	-	475	No	6.91
[24]	PV + BAT	370	31	11 h	-	Yes	7.22
[25]	BAT + H2	6000	200	-	130	No	16.6
[26]	BAT + H2	120	-	-	-	No	-
[27]	H2	250	250	-	-	No	-

2. Materials and Methods

To demonstrate the capabilities of hydrogen hybridization in electric urban transport versus battery-based technology, two unipersonal vehicles were designed: a battery-powered unipersonal electric vehicle and a hydrogen-based unipersonal electric vehicle. The goal was to mount the battery-based and the hydrogen-based powertrains on similar platforms and ensuring the total weight of the unipersonal electric vehicle was the same in both cases. Figure 1 shows the platform built with an iron chassis including all the components of the propulsion system. It should be noted that the hydrogen used in these facilities was green hydrogen, produced from renewable sources [28–30].

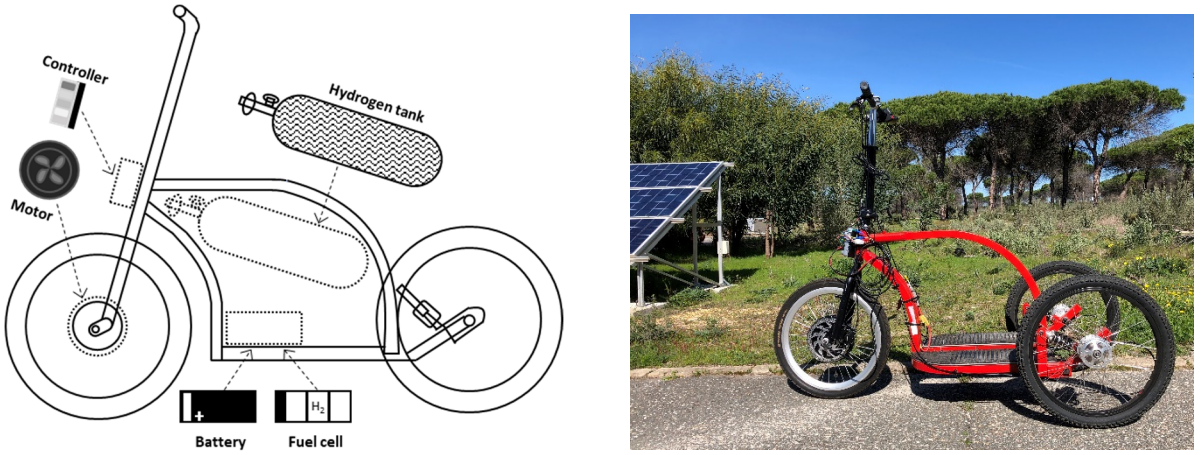

Figure 1. Unipersonal electric vehicle platform: (**a**) conceptual design; (**b**) physical implementation.

The platform integrated an electric motor of 24 V and 250 W by Golden Motor®, model MP3-20F Magic Pie® 3, attached to the front 20-inch wheel. It was sized in a range to meet the typical energy requirements in commercial batteries and fuel cells [31–34], promoting design scalability. The system was regulated through the programmable controller, model Magic® MX25 BAC-281P by Golden Motor®. System specifications are summarized in Table 2.

Table 2. Motor system specifications.

Device	Parameter	Value
Motor	Voltage (V) Power (W) Weight including wheel (kg)	24 250 7.5
Wheel	Size (cm)	50.8
Brushless motor controller	Voltage ranges (V) Max. power (W)	24, 36, 48 1000

2.1. Battery-Powered Unipersonal Electric Vehicle Configuration

The first design was based on the implementation of an electric unipersonal vehicle powered by battery, Figure 2 The motor, managed though its controller C_M, receives the necessary current directly from the battery, and the motor operating voltage matches with battery nominal voltage. In addition to the specific parameters previously described, motor voltage V_{motor}, current I_{motor} and battery current I_{bat} were monitored. Battery technical characteristics are summarized in Table 3.

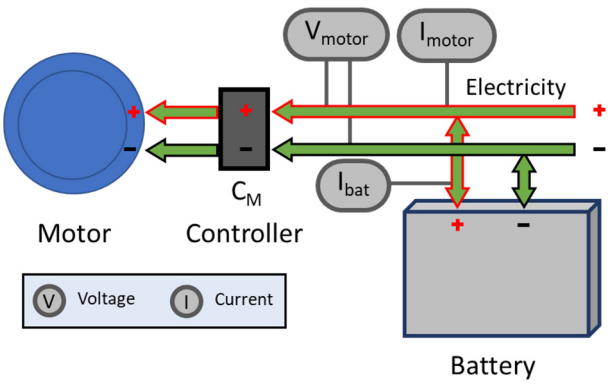

Figure 2. Battery-based propulsion system.

Table 3. Battery technical characteristics.

Parameter	Value
Model	Herewin MG-12000P
Nominal Voltage (V)	24 V
Rated Energy (Wh)	266
Capacity (Ah)	12
Weight (kg)	3.6
Technology	LiPo

2.2. Hydrogen-Powered Unipersonal Electric Vehicle Configuration

The hydrogen-based propulsion system bases its energy input on hydrogen technology together with a buffer battery, Figure 3.

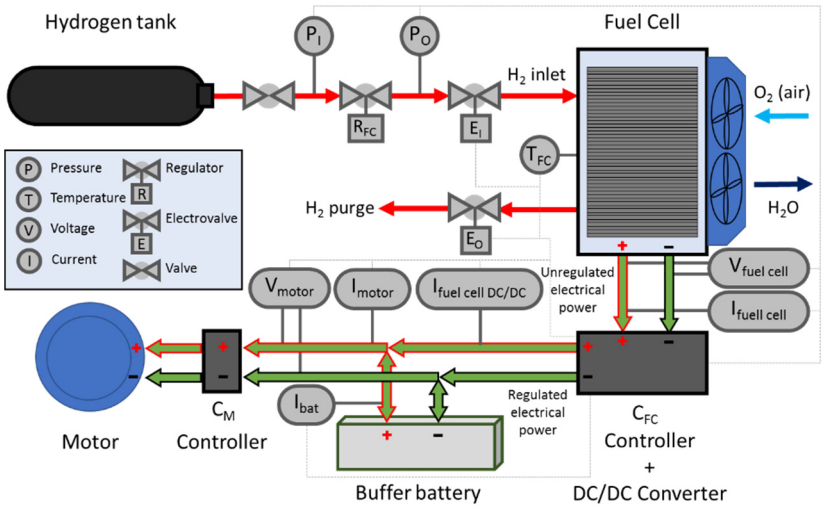

Figure 3. Hybridized hydrogen-based propulsion system.

The hydrogen-powered unipersonal electric vehicle has a hydrogen storage tank able to store up to 7 L, at a maximum pressure of 350 bar. The pressure of the stored hydrogen is reduced through the regulator R_{FC}. This reduction is carried out to adapt the hydrogen to the range of inlet pressure in the fuel cell. The selected fuel cell was the BMPower® 500, with a nominal power of 500 W. Due to commercial availability and cost/nominal power effective ratio, this model was the most suitable according to the requirements of the application (the objective is to compare two platforms with similar weight). To guarantee a safe operation, both inlet pressure, P_I, and output pressure, P_O, obtained at the ends of the regulator were monitored.

To allow hydrogen flow into the fuel cell, the inlet solenoid valve, E_I, is activated. The fuel cell produces electricity and water, from hydrogen and oxygen. A fan was used to blow the air from outside to provide oxygen to the cathode and to cool the fuel cell.

The electricity produced by the fuel cell passes through a DC/DC power converter that, through the controller C_{FC}, regulates the output according to the power demanded by the motor and the buffer battery's state of charge. The integration of the buffer battery aims to provide greater specific power and flexibility to the system in the face of demand peaks from the motor.

The motor controller, C_M, is based on the electromechanical systems of the electric vehicle, which are accelerator and brake. The fuel cell controller, C_{FC}, monitors hydrogen pressures P_I and P_O, fuel cell temperature T_{FC}, fuel cell voltage $V_{fuel\ cell}$, fuel cell current before the converter $I_{fuel\ cell}$ and after the converter $I_{fuel\ cell\ DC/DC}$, buffer battery current I_{bat}, motor voltage V_{motor}, and motor current I_{motor}. Based on these variables, and the operating instructions, the controller acts on the hydrogen inlet, E_I, to supply the hydrogen to the fuel cell, and on the purge solenoid valve, E_O, to periodically purge the hydrogen

not consumed by the fuel cell, ventilation system and air supply, and establishes a power command for the output of the DC/DC converter.

These parameters were monitored through a Wi-Fi connection and recorded during the experimental tests of the system. The BM Power® software tool is intended for monitoring and controlling the operation of the propulsion system, Figure 4. Technical specifications of the hybrid propulsion system are shown in Table 4

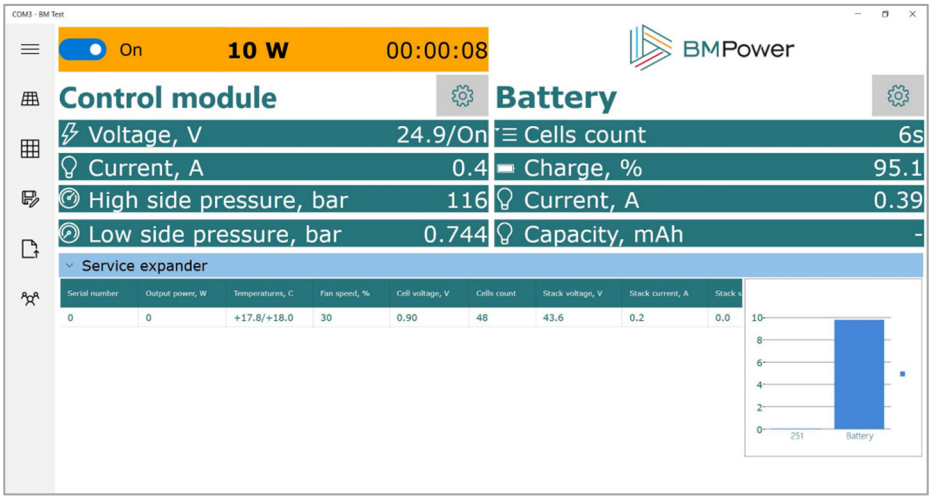

Figure 4. Control system software interface.

Table 4. Hybridized hydrogen-based propulsion system technical specifications.

Device	Parameter	Value
Storage tank	Volume (L)	7
	Weight (kg)	2.3
	Dimensions with regulator (mm)	Ø148 × 600
Fuel Cell	Model	BMPower® 500
	Rated Supply Voltage (V)	25–50
	Nominal Power (W)	500
	Dimensions with controller (mm)	225 × 145 × 124
	Weight including fan, controller and converter (kg)	1.1
	Cells	48
Controller + DC/DC converter	Rated Supply Voltage (V)	10–30
	Topology	Three synchronized lowering converters
Fan	Model	San Ace® 80 9G0824H101
	Voltage (V)	24
	Current (A)	0.42
	Power (W)	10.1
Buffer battery	Rated Supply Voltage (V)	22.2
	Rated Energy (Wh)	73
	Capacity (Ah)	3.3
	Weight (kg)	0.5
	Technology	LiPo
Wiring and piping	Weight (kg)	07

2.3. Physical Implementation—Battery vs. Hydrogen Technology Comparison

Figure 5 shows the physical implementation of the battery-based and the hybridized hydrogen-based unipersonal electrical vehicle. Both were implemented in the same platform, with an arrangement that allowed the pilot to manage and guaranteed an adequate air flow for correct ventilation and air supply.

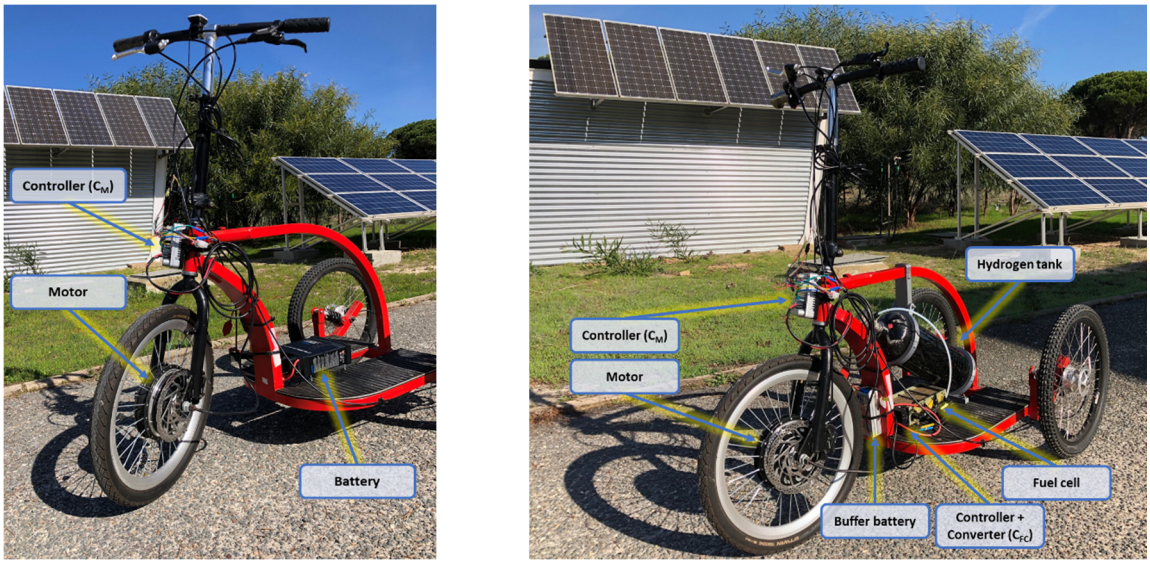

(**a**) (**b**)

Figure 5. System implementation: (**a**) battery-based unipersonal electric vehicle; (**b**) hydrogen-based unipersonal electric vehicle.

The technology comparison was carried out regarding the energy capacity of each design.

The specific energy supplied by the battery-based system is calculated by applying Equation (1):

$$e_{battery} = \frac{E_{battery}}{m_{battery}} \quad (1)$$

where:

$$E_{battery}\ (\text{Battery energy}) = 266\ \text{Wh};$$
$$m_{battery}\ (\text{Battery mass}) = 3.6\ \text{kg}.$$

Then, the battery specific energy is 74 Wh/kg.

In the hydrogen-based system, to calculate the specific energy it is necessary to know the amount of hydrogen stored in the tank. The hydrogen moles number, n_{H2}, can be obtained from Equation (2):

$$n_{H2} = \frac{p \cdot V}{Z \cdot R \cdot T} \quad (2)$$

where:

$$p\ (\text{Pressure}) = 3.5 \times 10^7\ \text{Pa};$$
$$V\ (\text{Volume}) = 0.007\ \text{m}^3;$$
$$Z\ (\text{Compressibility factor for 350 bar and 298.15 K}) = 1.25205;$$
$$R\ (\text{Ideal gas constant}) = 8.314472\ \tfrac{m^3 \cdot Pa}{K \cdot mol};$$
$$T\ (\text{Temperature}) = 298.15\ \text{K}.$$

Therefore, the hydrogen tank provides 78.9359 mol of H_2.

To obtain the hydrogen energy, hydrogen properties considered are:

HHV_{H2} (hydrogen higher heating value) = 141.86 MJ/kg.

The hydrogen energy provided is 6221 Wh; and the hydrogen specific energy supplied is obtained by applying Equation (3):

$$e_{H2} = \frac{E_{H2}}{m_{H2}} \quad (3)$$

where:

$$E_{H2}\ (\text{Hydrogen energy}) = 6221\ \text{Wh};$$
$$m_{H2}\ (\text{Hydrogen system mass}) = 4.2\ \text{kg}.$$

Then, the hydrogen specific energy provided is 1481 Wh/kg.

The hybridized hydrogen-based system also included a buffer battery of 73 Wh and 0.5 kg. Applying the Equation (1), the buffer battery specific energy is 146 Wh/kg, while full hybrid system specific energy is 1339 Wh/kg.

Additionally, to compare the energy–volume relation in both powertrains, it is necessary to know the whole volume of each system. The battery-based powertrain volume is 2139 cm^3. In the hydrogen-based powertrain, the tank volume is 7958 cm^3, fuel cell volume is 3289 cm^3 and buffer battery volume is 243 cm^3. Therefore, the battery-based powertrain energy-volume relation is 124,357 Wh/m^3, while in the hydrogen-based powertrain the relation is 541,426 Wh/m^3.

Quantitative comparison of both platforms is shown in Table 5; improvements were verified both in specific energy and energy–volume relation for the hydrogen-based design. This can be quantified as an increase of 1790% in specific energy and 335% in energy–volume relation.

Table 5. Battery vs. hydrogen technology comparison.

Powertrain System	Energy (Wh)	Specific Energy (Wh/kg)	Energy-Volume (Wh/m^3)	Volume (cm^3)	Autonomy (km) *	Recharge Time (h)	Weight (kg)
Battery-powered	266	74	124,357	2139	15	4	3.6
Hydrogen-powered	6294	1339	541,426	11,490	290	0.03	4.7

*: Obtained from experimental road test, Section 3.4.

3. Results

To obtain the experimental data results, dynamic laboratory and dynamic road tests were carried out over the two configurations: battery-based and hydrogen-based unipersonal electric vehicle, Figure 6.

(**a**) (**b**)

Figure 6. Unipersonal electric vehicle test benches: (**a**) laboratory dynamic test; (**b**) road test.

The dynamic laboratory test consisted of applying acceleration over the motor, and then provoking friction or manual braking. For the dynamic road test, a real driving test was applied over the unipersonal electric vehicle in movement.

3.1. Experimental Test from Battery-Powered Unipersonal Vehicle

To check the battery-powered unipersonal vehicle platform, it was firstly subjected to a dynamic laboratory driving profile, Figure 7. Different acceleration stages were applied, causing friction or manual braking. As it can be observed, the battery current followed the motor current demand, $I_{bat} = -I_{motor}$ (authors considered a positive sign when current

was leaving the device, and negative sign when current was entering the device). State of charge [35] of the battery (SOC) was calculated applying Equation (4):

$$SOC(t) = SOC(t-1) + \frac{I(t)}{Q_n}\Delta t \quad (4)$$

where:

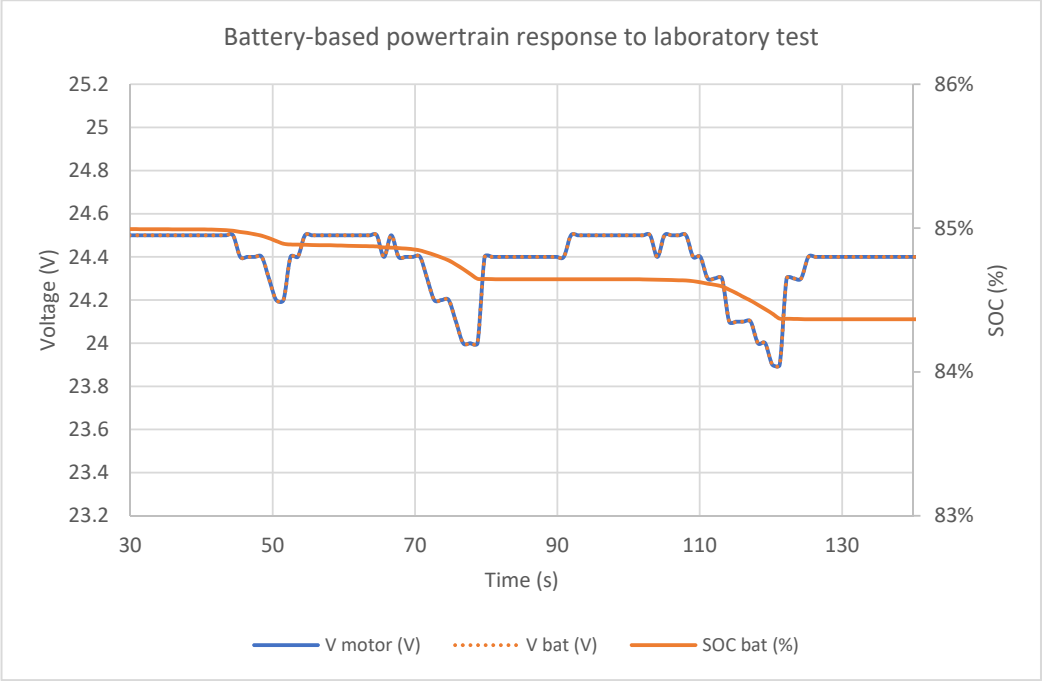

(**a**)

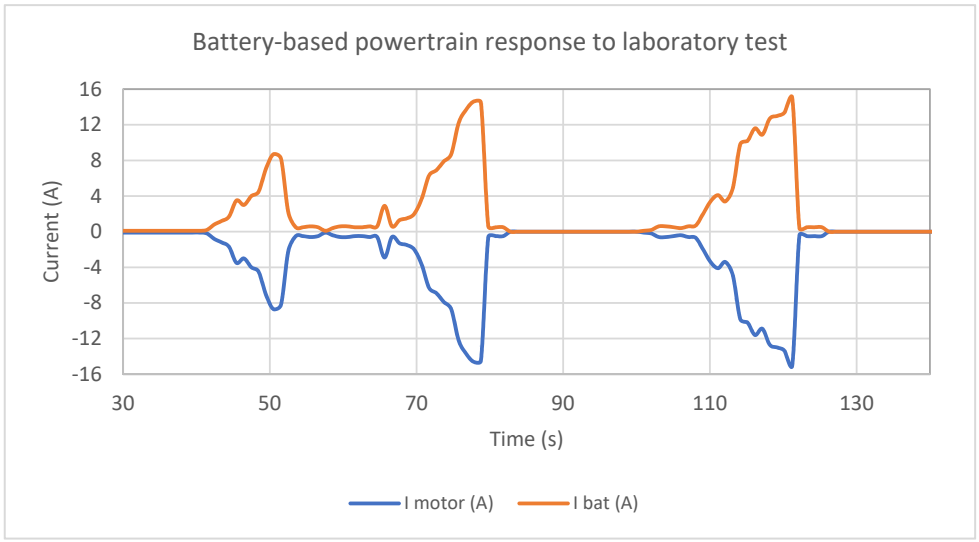

(**b**)

Figure 7. Battery-based unipersonal electric vehicle response to laboratory dynamic test: (**a**) motor and battery voltage and SOC vs. time; (**b**) battery and motor current vs. time. Initial condition: SOC = 85%.

$SOC(t)$ is state of charge in a time t;
$SOC(t-1)$ is the SOC at the previous instant;
$I(t)$ is the battery current (A);
Q_n is nominal capacity of the battery (Ah);
Δt is time differential (s).

The second test consisted of an evaluation of the battery-based unipersonal electric vehicle behavior, when it was put on-road. Battery supplied the motor demand, and as a consequence, the battery SOC decreased with time, Figure 8.

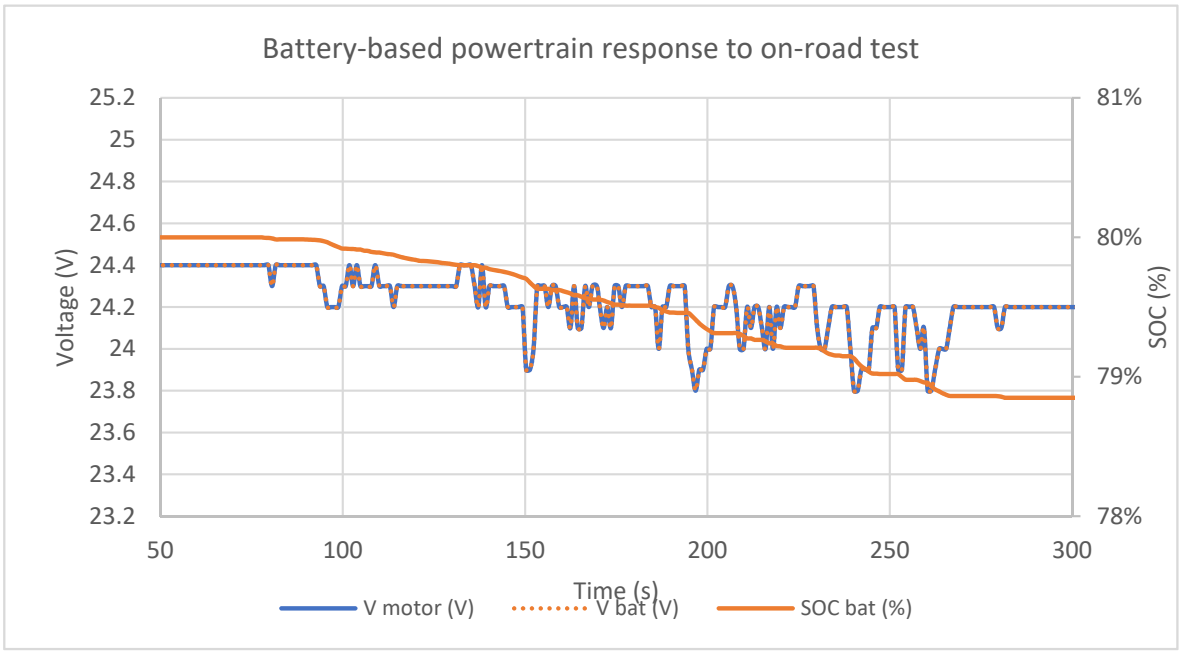

(**a**)

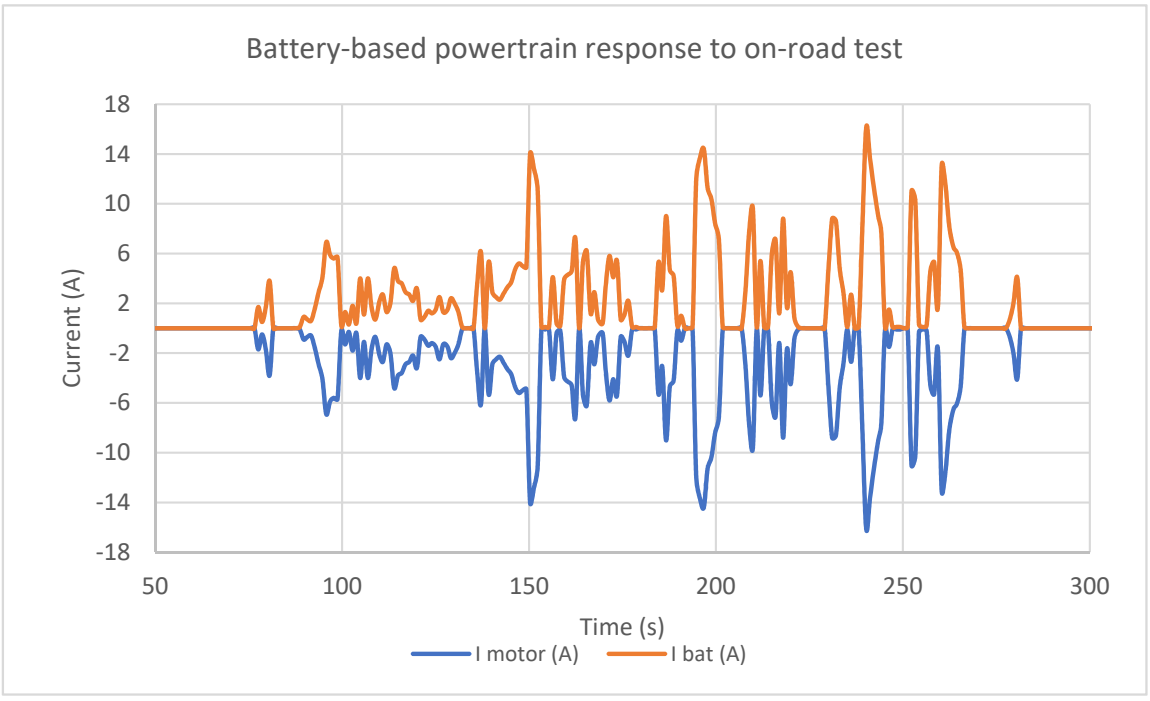

(**b**)

Figure 8. Battery-based unipersonal electric vehicle response to on-road dynamic test: (**a**) motor voltage and battery voltage and SOC vs. time; (**b**) battery and motor current vs. time. Initial condition: SOC = 80%.

3.2. Experimental Test from Hydrogen-Powered Unipersonal Vehicle

In this case, the test consisted of evaluating the unipersonal electric vehicle behavior when the powertrain was hybridized with a fuel cell and the battery. As demonstrated

above, in the first test, the hybrid hydrogen-based unipersonal vehicle was subjected to a laboratory dynamic driving profile. This test observed the initial current hybridization between the fuel cell current and the buffer battery current to satisfy the current demanded by the motor. The motor voltage was fixed by the battery (nominal voltage 24 V), and the fuel cell converter acted as step-down stage (fuel cell voltage varied between 42.2 V and 33.2 V, and it reduced to 24 V). Based on the difference between the motor demand and the maximum current supplied by the fuel cell, the controller varied the converter duty-cycle with the aim to put the fuel cell into the appropriate operating point.

When the motor demand was lower than the maximum fuel cell current, the controller adjusted the DC/DC converter to put the fuel cell operating at the point that satisfies the motor demand, and the remaining current was used to recharge the battery ($I_{bat} = -1$ A), Figure 9. Note that the fuel cell provided almost all of the motor current demand. Sudden changes in the demand were reflected in the fuel cell. The battery filtered instabilities and provided current peaks when the demand was higher than the fuel cell nominal current. Through the test, as the battery absorbed current from fuel cell, the battery SOC increased gradually. Hydrogen was consumed, so the pressure in the tank was reduced. Power balance can be at each operating point; for example, at t = 12,000 s, $I_{fuelcell} = 4.2$ A, which converted to I_{fuel} cell DC/DC = 5.1 A. Fuel cell converter output current was consumed by the motor ($I_{motor} = -4.1$ A) and the battery ($I_{bat} = -1$ A).

The last test consisted of an on-road dynamic test to assess the capability of the designed powertrain in meeting the requirements of a real driving profile, Figure 10.

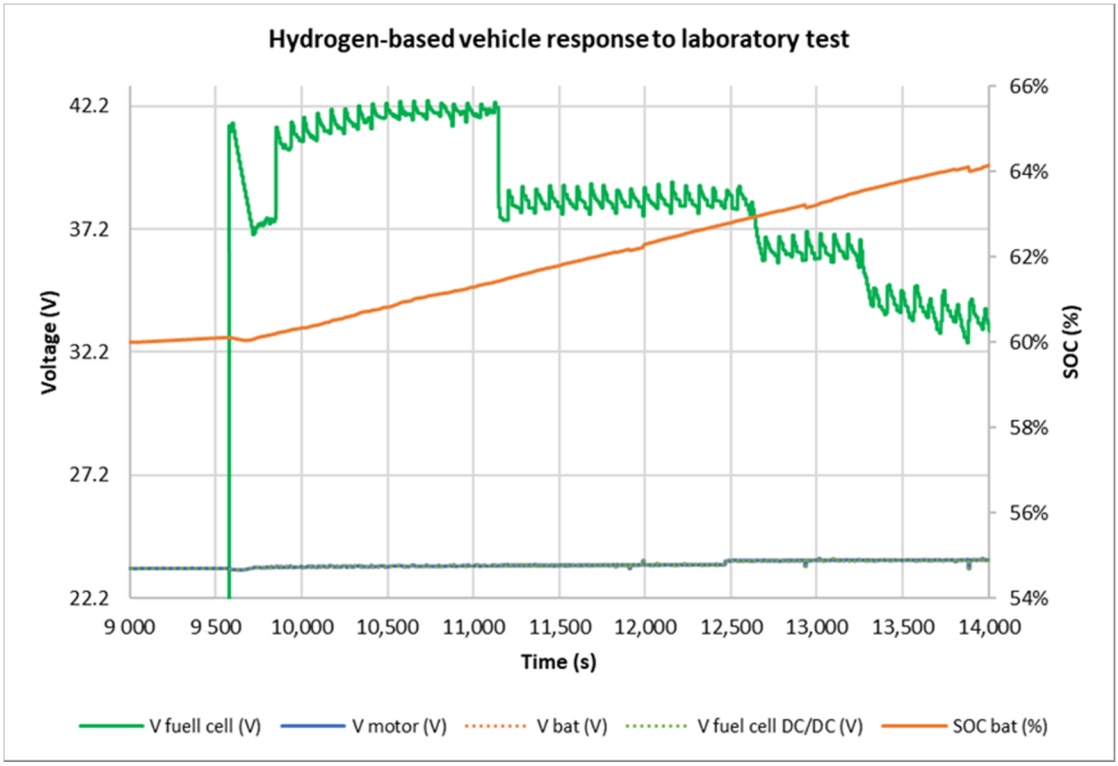

(**a**)

Figure 9. *Cont.*

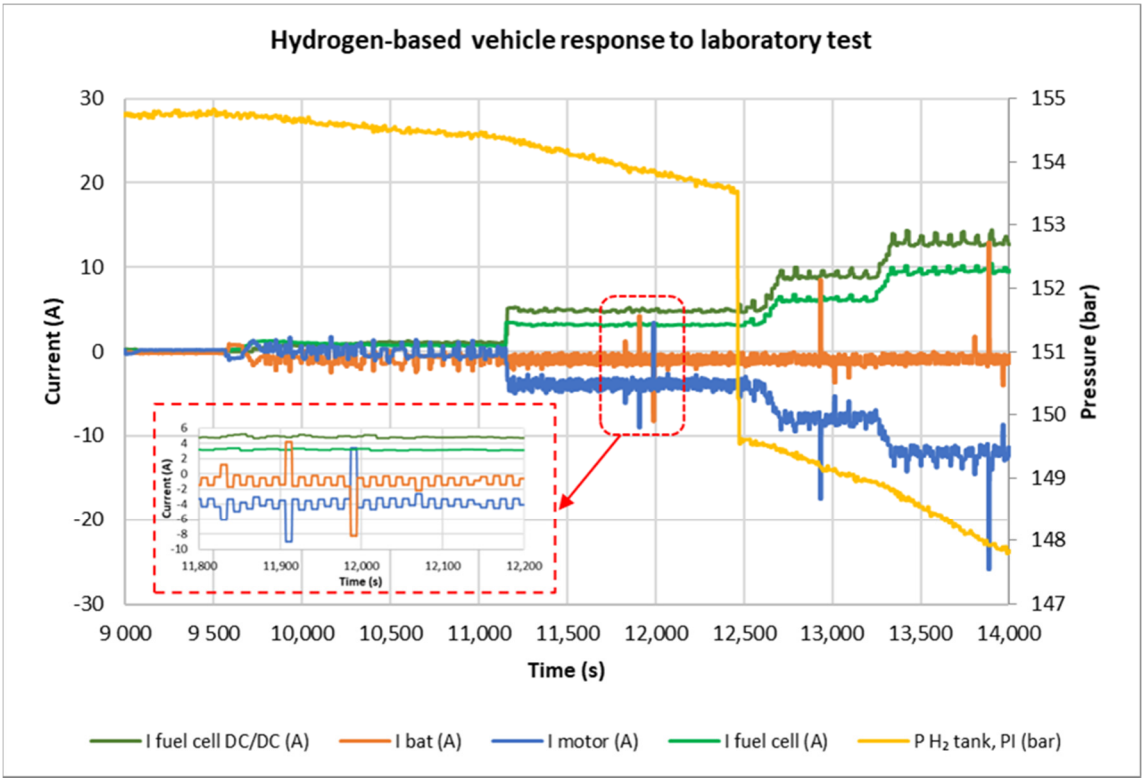

(**b**)

Figure 9. Hydrogen-based unipersonal electric vehicle response to laboratory dynamic test. (**a**) Motor and fuel cell voltages and battery SOC vs. time; (**b**) fuel cell, motor, battery currents and pressure vs. time. Initial condition: SOC = 60%; H2 Pressure = 154.6 bar.

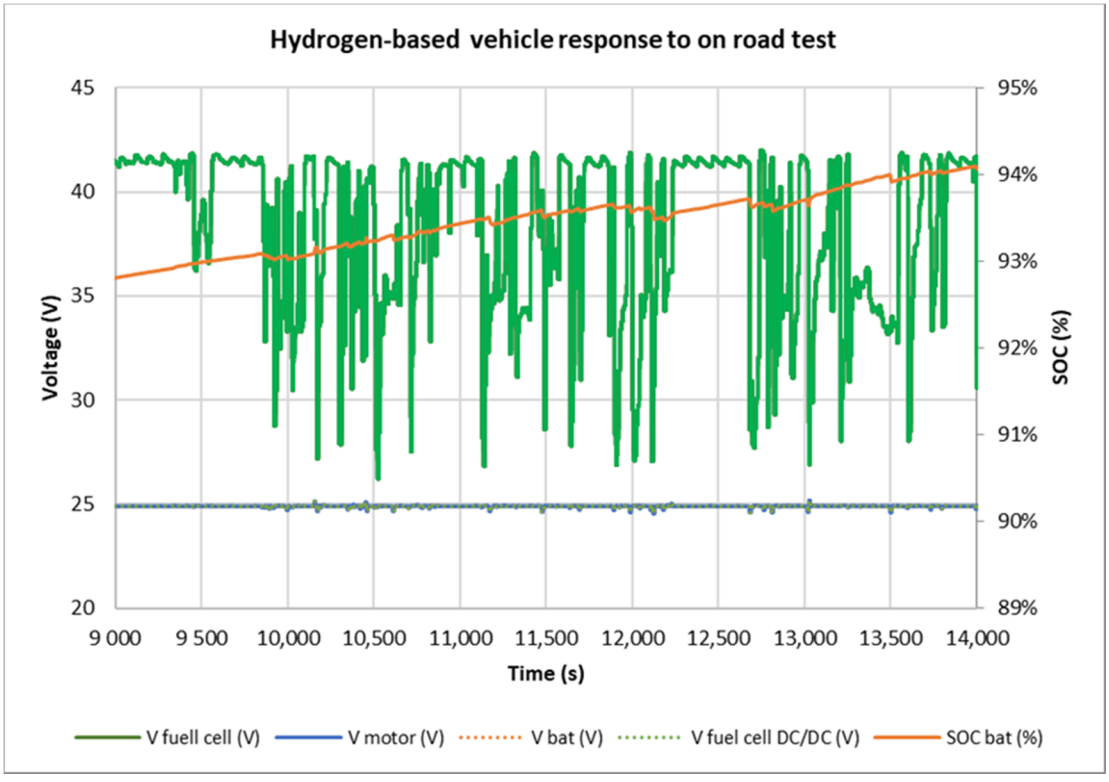

(**a**)

Figure 10. *Cont.*

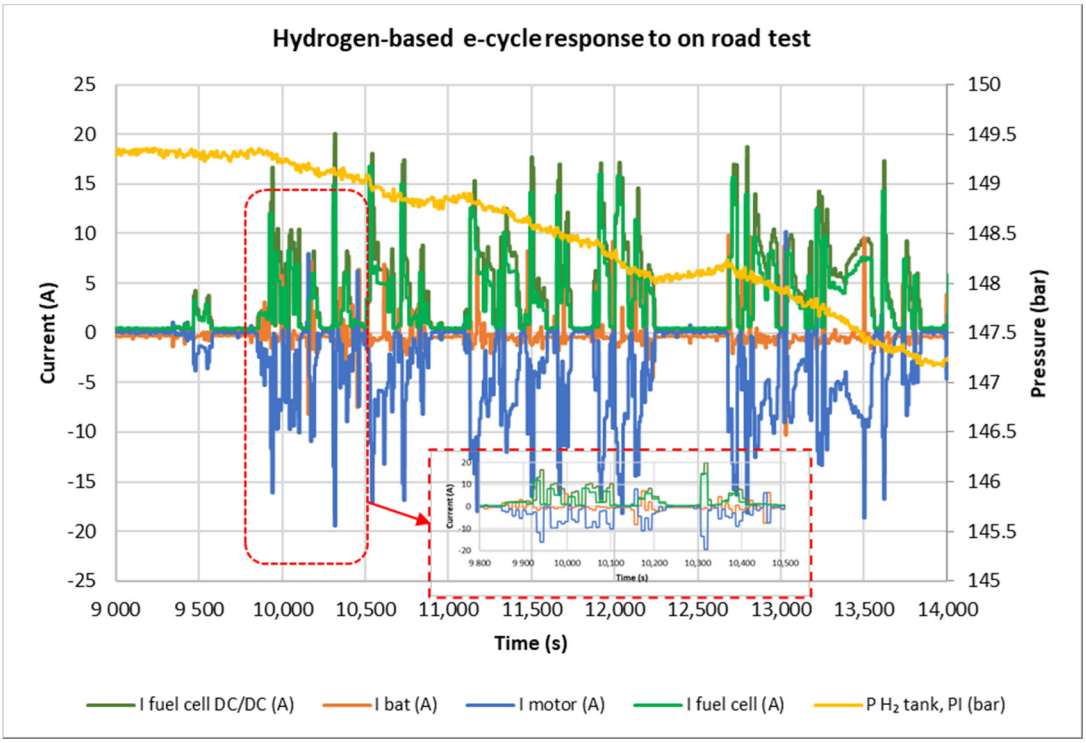

(**b**)

Figure 10. Hydrogen-based unipersonal electric vehicle response to on-road dynamic test: (**a**) fuel cell, motor, battery voltages and SOC vs. time; (**b**) fuel cell, motor, battery currents and pressure vs. time. SOC = 93%; initial pressure = 149.3 bar.

In this test, the hydrogen-based powertrain was subjected to sudden changes in the driving profile. Note that the fuel cell provided almost all the current while the battery filtered instabilities and provided current peaks. Battery SOC started at 93%, as it was continuously charging, meanwhile it did not provide the required current peaks. When motor current peaks needed to be provided by the battery, its SOC decreased instantaneously. Hydrogen pressure in the storage tank reduced and can be measured to later estimate the autonomy of the system. Overall, the fuel cell responded with enough power to meet the motor demand and to charge the battery, validating the hybrid design along the buffer battery.

3.3. Temperature Test

During the on-road tests of the hybridized hydrogen-based unipersonal electric vehicle, it was verified that the temperature remained in an adequate range, with the corresponding increase in the fan speed for cooling during higher peaks of current supplied by the fuel cell. Although the system guarantees good cooling, it is interesting to consider innovative solutions in battery cooling [36] to scale the hybrid propulsion system to higher power developments. The temperature evolution during on-road test according to the current and the fan interaction is verified in Figure 11.

3.4. On-Road Autonomy Test

The on-road autonomy test covered a total of 48 km at an average speed of 12 km/h. The unipersonal electric vehicle was first operated with battery-based powertrain and then with hydrogen-based powertrain, on a bicycle path, from INTA facilities to the town of Mazagón. Taking into account the hydrogen-based system, initially the hydrogen pressure tank achieved 350 bar. At the end of the test, pressure was reduced 68 bar. Using the Redlkich–Kwong equation of state [37], a hydrogen consumption of 26.5 g was obtained, assuming that the tank was at 25 °C during the entire test. This resulted in an energy

consumption of 1044 Wh (HHV). On the other hand, according to Table 5, Section 2.3, the total amount of energy available in hydrogen-based system was 6294 Wh (HHV), and 266 Wh in battery-based system. This means there was a maximum autonomy of 290 km for the hydrogen-based system while just 15 km for the battery-based system.

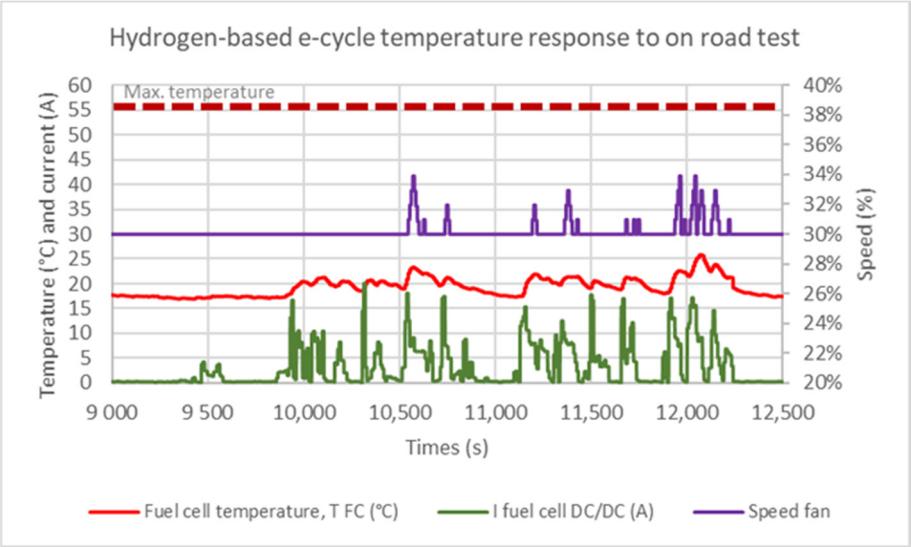

Figure 11. Hydrogen-based hybrid electric vehicle temperature response to on-road dynamic test.

4. Discussion

This section presents an analysis of the main results obtained in the tests. Both battery-based and hydrogen-based unipersonal electric vehicles developed in this work have been exposed to real laboratory and on-road driving test conditions, according to the urban mobility conditions for which they have been developed.

4.1. Battery-Based System Response

The battery system has a direct energy exchange between the motor demand and the battery supply. In this way, as the motor accelerates, it demands more electrical current, supplied directly from the electrical energy stored in the battery. This causes a reduction in the battery SOC and, thus, the battery voltage. The system limits its flexibility to that provided by the characteristics of the battery. Therefore, for a battery-based unipersonal electric vehicle, it must be scaled based on the selected battery since the entire propulsion system—acceleration, autonomy, recharging, etc.—is directly linked to the battery selection.

4.2. Hydrogen-Based System Response

In the hydrogen-based hybrid system, in response to the demand of the motor, there is a stabilized supply from the fuel cell, through its DC/DC converter. In this system, the battery acts as a buffer, providing current and energy, in cases where the fuel cell is not able to supply instantaneous high current demand peaks from the motor. Slow motor demand transients can be supplied by the fuel cell. In short transient demand peaks, the battery supplies the necessary current. Likewise, the battery undergoes instantaneous SOC decreases, which are recovered in the next driving step. Regarding the hydrogen consumption, it also decreases the pressure in the hydrogen tank as it is consumed by the fuel cell for the electricity production. Therefore, the system shows an energy flexibility scalable to the supply capacity of the hydrogen system. The greater the storage tank capacity, the greater the autonomy, the larger the fuel cell and its converter, and the more energy that can be supplied directly. Power flexibility depends not only on the hydrogen system, but also on the buffer battery. Once it has been verified that it provides the current peaks demanded by the motor, it must be scaled based on the corresponding urban mobility application.

5. Conclusions

In this work, a test platform was built to establish a comparison between a unipersonal electric vehicle powered only by batteries, and the same one powered by a hybrid system based on hydrogen and batteries. Both systems had similar weight. In this way, it is possible to compare both technologies, their advantages and disadvantages, in the same platform. The autonomy of the hybrid hydrogen-based system was 290 km, being much greater than that of the battery-based system that reached approximately 15 km. Preliminary conclusions allow us to recognize that energy hybridization provides great specific advantages to urban mobility applications. Indeed, the improvements can be quantified as an increase of 1790% in specific energy and 335% in energy–volume relation. The results show that the unipersonal electric vehicle equipped with a hydrogen-based powertrain provides not only greater autonomy, but also has shorter recharge times.

The capacities obtained in terms of autonomy, recharging time and, above all, environmental advantages regarding the reduction in pollutants, make this a promising and scalable proposal for use in sustainable cities.

Author Contributions: Conceptualization, F.I.L. and F.S.M.; methodology, F.I.L., J.M.A., E.L.G. and F.S.M.; validation, J.J.C.M. and E.L.G.; formal analysis, F.I.L. and F.S.M.; investigation, All; resources, F.I.L. and E.L.G.; data curation, J.J.C.M.; writing—original draft preparation, F.I.L. and J.J.C.M.; writing—review and editing, All; supervision, J.M.A. All authors have read and agreed to the published version of the manuscript.

Funding: This research received no external funding.

Institutional Review Board Statement: Not applicable.

Informed Consent Statement: Not applicable.

Data Availability Statement: Not applicable.

Acknowledgments: The authors would like to thank Manuel Gil for his helpful advice in various technical issues regarding the testing platform.

Conflicts of Interest: The authors declare no conflict of interest.

List of Acronyms

BAT	Battery
DC	Direct current
FC	Fuel cell
HHV	Higher heating value
SOC	State of charge

Notation and Symbols

C-rates	charge/discharge rates
Δt	time differential (s)
$E_{battery}$	Battery energy (Wh)
E_{H2}	Hydrogen energy (Wh)
$e_{battery}$	Battery specific energy (Wh/kg)
e_{H2}	Hydrogen system specific energy (Wh/kg)
$I(t)$	Discharging current (A)
$m_{battery}$	Battery mass (kg)
m_{H2}	Hydrogen system mass (kg)
n_{H2}	number of hydrogen mol (mol)
p	Pressure (Pa)
Q_n	Nominal capacity (Ah)
T	Temperature (K)
V	Volume (m^3)
HHV_{H2}	Hydrogen higher heating value (141.86 MJ/kg)
R	Ideal gas constant (8.314472 $m^3 \cdot Pa/K \cdot mol$)
Z	Hydrogen Compressibility factor at 350 bar and 298.15 K (1.25205)

References

1. Urban Population (% of Total Population) | Data. Available online: https://data.worldbank.org/indicator/SP.URB.TOTL.IN.ZS?end=2019&name_desc=false&start=1960&view=chart (accessed on 28 January 2021).
2. Jenelius, E.; Cebecauer, M. Impacts of COVID-19 on public transport ridership in Sweden: Analysis of ticket validations, sales and passenger counts. *Transp. Res. Interdiscip. Perspect.* **2020**, *8*, 100242. [CrossRef]
3. Thurston, G.D. Outdoor Air Pollution: Sources, Atmospheric Transport, and Human Health Effects. In *International Encyclopedia of Public Health*; Elsevier BV: Amsterdam, The Netherlands, 2017; pp. 367–377.
4. Redman, C. The Impact of Motorcycles on Air Quality and Climate Change: A Study on the Potential of Two-Wheeled Electric Vehicles. Senior Thesis, Claremont McKenna College, Claremont, CA, USA, 2015.
5. Diaz-Cachinero, P.; Munoz-Hernandez, J.I.; Contreras, J. A Linear Model for Operating Microgrids with Renewable Resources, Battery Degradation Costs and Electric Vehicles. In Proceedings of the 2018 15th International Conference on the European Energy Market (EEM), Lodz, Poland, 27–29 June 2018; Volume 2018, pp. 1–5.
6. Wang, S.; Guo, D.; Han, X.; Lu, L.; Sun, K.; Li, W.; Sauer, D.U.; Ouyang, M. Impact of battery degradation models on energy management of a grid-connected DC microgrid. *Energy* **2020**, *207*, 118228. [CrossRef]
7. Qiao, D.; Wang, G.; Gao, T.; Wen, B.; Dai, T. Potential impact of the end-of-life batteries recycling of electric vehicles on lithium demand in China: 2010–2050. *Sci. Total. Environ.* **2021**, *764*, 142835. [CrossRef]
8. Ryan and Phil. Events with Smoke, Fire, Extreme Heat, Or Explosion Involving Lithium Batteries. Available online: https://www.faa.gov/hazmat/resources/lithium_batteries/media/Battery_incident_chart.pdf (accessed on 18 May 2021).
9. Safety Concerns with Li-ion Batteries-Battery University. Available online: https://batteryuniversity.com/learn/article/safety_concerns_with_li_ion (accessed on 18 May 2021).
10. Larsson, F.; Andersson, P.; Blomqvist, P.; Mellander, B.-E. Toxic fluoride gas emissions from lithium-ion battery fires. *Sci. Rep.* **2017**, *7*, 1–13. [CrossRef] [PubMed]
11. Minakshi, M.; Higley, S.; Baur, C.; Mitchell, D.R.G.; Jones, R.; Fichtner, M. Calcined chicken eggshell electrode for battery and supercapacitor applications. *RSC Adv.* **2019**, *9*, 26981–26995. [CrossRef]
12. Minakshi, M.; Mitchell, D.R.G.; Jones, R.; Pramanik, N.C.; Jean-Fulcrand, A.; Garnweitner, G. A Hybrid Electrochemical Energy Storage Device Using Sustainable Electrode Materials. *ChemistrySelect* **2020**, *5*, 1597–1606. [CrossRef]
13. Mancera, J.J.C.; Manzano, F.S.; Andújar, J.M.; Vivas, F.J.; Calderón, A.J. An Optimized Balance of Plant for a Medium-Size PEM Electrolyzer: Design, Control and Physical Implementation. *Electronics* **2020**, *9*, 871. [CrossRef]
14. Chen, H.-S.; Tsai, B.-K.; Hsieh, C.-M. Determinants of Consumers' Purchasing Intentions for the Hydrogen-Electric Motorcycle. *Sustainability* **2017**, *9*, 1447. [CrossRef]
15. Chen, H.-S.; Tsai, B.-K.; Hsieh, C.-M. The Effects of Perceived Barriers on Innovation Resistance of Hydrogen-Electric Motorcycles. *Sustainability* **2018**, *10*, 1933. [CrossRef]
16. Handa, K.; Yamaguchi, S.; Minowa, K.; Mathison, S. Development of New Hydrogen Fueling Method for Fuel Cell Motorcycle. *SAE Int. J. Altern. Powertrains* **2017**, *6*, 219–227. [CrossRef]
17. Weigl, J.D.; Henz, M.; Inayati; Saidi, H. Converted battery-powered electric motorcycle and hydrogen fuel cell-powered electric motorcycle in South East Asia: Development and performance test. In Proceedings of the Joint International Conference on Electric Vehicular Technology and Industrial, Mechanical, Electrical and Chemical Engineering (ICEVT & IMECE), Surakarta, Indonesia, 4–5 November 2015; pp. 1–4.
18. Di Trolio, P.; Di Giorgio, P.; Genovese, M.; Frasci, E.; Minutillo, M. A hybrid power-unit based on a passive fuel cell/battery system for lightweight vehicles. *Appl. Energy* **2020**, *279*, 115734. [CrossRef]
19. Li, M.; Bai, Y.; Zhang, C.; Song, Y.; Jiang, S.; Grouset, D.; Zhang, M. Review on the research of hydrogen storage system fast refueling in fuel cell vehicle. *Int. J. Hydrogen Energy* **2019**, *44*, 10677–10693. [CrossRef]
20. Paudel, A.M.; Kreutzmann, P. Design and performance analysis of a hybrid solar tricycle for a sustainable local commute. *Renew. Sustain. Energy Rev.* **2015**, *41*, 473–482. [CrossRef]
21. Pios hydrogen fuel cell tricycle. *Int. J. Hydrogen Energy* **2005**, *30*, 1035–1036. [CrossRef]
22. Devan, P.; Bibin, C.; Krrishana, A.G.; Ashwin, M.; Kumar, K.B.; Dinesh, K. A comprehensive review on solar tricycles. In Proceedings of the Materials Today: Proceedings; Elsevier BV: Amsterdam, The Netherlands, 2020; Volume 33, pp. 229–231.
23. Piumsomboon, P.; Pruksathorn, K.; Hunsom, M.; Tantavichet, N.; Charutawai, K.; Kittikiatsophon, W.; Nakrumpai, B.; Sripakagorn, A.; Damrongkijkarn, P. Road testing of a three-wheeler driven by a 5 kW PEM fuel cell in the absence and presence of batteries. *Renew. Energy* **2013**, *50*, 365–372. [CrossRef]
24. Masud, M.H.; Akhter, S.; Islam, S.; Parvej, A.M.; Mahmud, S. Design, Construction and Performance Study of a Solar Assisted Tri-cycle. *Period. Polytech. Mech. Eng.* **2017**, *61*, 234. [CrossRef]
25. Lin, B. Conceptual design and modeling of a fuel cell scooter for urban Asia. *J. Power Sources* **2000**, *86*, 202–213. [CrossRef]
26. De León, C.P.; Walsh, F.; Patrissi, C.; Medeiros, M.; Bessette, R.; Reeve, R.; Lakeman, J.; Rose, A.; Browning, D. A direct borohydride–peroxide fuel cell using a Pd/Ir alloy coated microfibrous carbon cathode. *Electrochem. Commun.* **2008**, *10*, 1610–1613. [CrossRef]
27. Masterflex, Veloform link for fuel cell bikes. *Fuel Cells Bull.* **2004**, *2004*, 4. [CrossRef]
28. López, E.; Isorna, F.; Rosa, F. Optimization of a solar hydrogen storage system: Exergetic considerations. *Int. J. Hydrogen Energy* **2007**, *32*, 1537–1541. [CrossRef]

29. González, E.L.; Llerena, F.I.; Pérez, M.S.; Iglesias, F.R.; Macho, J.G. Energy evaluation of a solar hydrogen storage facility: Comparison with other electrical energy storage technologies. *Int. J. Hydrogen Energy* **2015**, *40*, 5518–5525. [CrossRef]
30. López, E.; Isorna, F.; Rosa, F. Optimization of a Solar Hydrogen Storage System: Safety Considerations. In Proceedings of the Conference WHEC16: 16, World Hydrogen Energy Conference, Lyon, France, 13–16 June 2006. INIS-FR-6794.
31. Hellmann, J.V.; Sandel, R.J. Dual/High Voltage Vehicle Electrical Systems. *SAE Tech. Paper Ser.* **1991**. [CrossRef]
32. Corbo, P.; Migliardini, F.; Veneri, O. Performance investigation of 2.4kW PEM fuel cell stack in vehicles. *Int. J. Hydrogen Energy* **2007**, *32*, 4340–4349. [CrossRef]
33. Lu, F.; Zhang, H.; Zhu, C.; Diao, L.; Gong, M.; Zhang, W.; Mi, C.C. A Tightly Coupled Inductive Power Transfer System for Low-Voltage and High-Current Charging of Automatic Guided Vehicles. *IEEE Trans. Ind. Electron.* **2018**, *66*, 6867–6875. [CrossRef]
34. Hamdan, M.M.; Holler, G.; Grolle, K.A.; Macnamara, J.M.; Thakkar, K.A. System and method for detecting alternator condition. Google Patents , Patent US 6,862,504 B2, 1 March 2005.
35. Chang, W.-Y. The State of Charge Estimating Methods for Battery: A Review. *ISRN Appl. Math.* **2013**, *2013*, 1–7. [CrossRef]
36. Divakaran, A.M.; Hamilton, D.; Manjunatha, K.N.; Minakshi, M. Design, Development and Thermal Analysis of Reusable Li-Ion Battery Module for Future Mobile and Stationary Applications. *Energies* **2020**, *13*, 1477. [CrossRef]
37. Tsonopoulos, C.; Heidman, J. From Redlich-Kwong to the present. *Fluid Phase Equilibria* **1985**, *24*, 1–23. [CrossRef]